COPY RIGHT

IJIEMR Transactions, online available on 10th January 2018. Link :

http://www.ijiemr.org/downloads.php?vol=Volume-7&issue=ISSUE-01

Paper Authors

* PAVANKALYAN, M.V.BINDHU.

* Dept of EEE, Tudi Ramreddy Institute of Science and Technology.

USE THIS BARCODE TO ACCESS YOUR ONLINE PAPER

To Secure Your Paper As Per UGC Guidelines We Are Providing A Electronic Bar Code

PV-POWERED SRM DRIVE FOR EVS WITH ADAPTABLE ENERGY CONTROL FUNCTIONS

*PAVANKALYAN, **M.V.BINDHU

*PG Scholar, Dept of EEE, Tudi Ramreddy Institute of Science and Technology

**Assistant Professor, Dept of EEE, Tudi Ramreddy Institute of Science and Technology

ABSTRACT:

Electric vehicles (EVs) provide a feasible solution to reducing greenhouse gas emissions and thus become a hot topic for research and development. Switched reluctance motors (SRMs) are one of promised motors for EV applications. In order to extend the EVs' driving miles, the use of photovoltaic (PV) panels on the vehicle helps decrease the reliance on vehicle batteries. Based on phase winding characteristics of SRMs, a tri-port converter is proposed in this paper to control the energy flow between the PV panel, battery and SRM. Six operating modes are presented, four of which are developed for driving and two for standstill on-board charging. In the driving modes, the energy decoupling control for maximum power point tracking (MPPT) of the PV panel and speed control of the SRM are realized. In the standstill charging modes, a grid-connected charging topology is developed without a need for external hardware. When the PV panel directly charges the battery, a multi-section charging control strategy is used to optimize energy utilization. Simulation results based on Matlab/Simulink and experiments prove the effectiveness of the proposed tri-port converter, which has potential economic implications to improve the market acceptance of Evs
.

INTRODUCTION

Electric vehicles (EVs) have taken a significant leap forward by advances in motor drives, power converters, batteries, and energy management systems. However, due to the limitation of current battery technologies, the driving miles are relatively short that restricts the wide application of EVs . In terms of motor drives, high-performance permanent-magnet (PM) machines are widely used while rare earth materials are needed in large quantities, limiting the wide application of EVs

In order to overcome these issues, a photovoltaic (PV) panel and a switched reluctance motor (SRM) are introduced to provide power supply and motor drive, respectively. First, by adding the PV panel on top of the EV, a sustainable energy source is achieved. Nowadays, a typical passenger car has a surface enough to install a 250-W PV panel. Second, a SRM needs no rare-earth PMs and is also robust so that it receives increasing attention in EV applications. While PV panels have low-power density for traction drives, they can be used to charge batteries most of time. Generally, the PV-fed EV has a

similar structure to the hybrid electrical vehicle (HEV), whose

internal combustion engine (ICE) is replaced by the PV panel. The PV-fed EV system is illustrated in Fig. 1. Its key components include an off-board charging station, a PV, batteries, and power converters. In order to decrease the energy conversion processes, one approach is to redesign the motor to include some on board charging functions. For instance, paper designs a 20-kW split-phase PM motor for EV charging, but it suffers from high harmonic contents in the back electromotive force (EMF). Another solution is based on a traditional SRM. Paper achieves onboard charging and power factor correction in a 2.3-kW SRM by employing machine windings as the input filter inductor. The concept of modular structure of driving topology is proposed in paper. Based on the intelligent power modules (IPMs), a four-phase half bridge converter is employed to achieve driving and grid-charging. Although modularization

supports mass production, the use of half/full

bridge topology reduces the system reliability (e.g., shoot-through issues). Paper develops a simple topology for plug-in HEV that supports flexible energy flow. But for grid-charging, the grid should be connected to the generator rectifier that increases the energy conversion process and decreases the charging efficiency. Nonetheless, an effective topology and control strategy for PV-fed EVs is not yet developed. Because the PV has different characteristics to ICEs, the maximum power point tracking (MPPT) and solar energy utilization are the unique factors for the PV-fed EVs.

In order to achieve low-cost and flexible energy flow modes, a low-cost tri-port converter is proposed in this paper to coordinate the PV panel, SRM, and battery. Six operational modes are developed to support flexible control of energy flow.
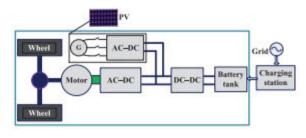

Fig. 1. PV-fed HEV.

PROPOSED CONCEPT
TOPOLOGY AND OPERATIONAL MODES

Proposed Topology and Working Modes

The proposed tri-port topology has three energy terminals, PV, battery, and SRM. They are linked by a power converter that consists of four switching devices (S_0 - S_3), four diodes (D_0 - D_3), and two relays, as shown in Fig. 2. By controlling relays J_1 and J_2, the six operation modes are supported, as shown in Fig. 3; the corresponding relay actions are illustrated in Table I. In mode 1, PV is the energy source to drive the SRM and to charge the battery. In mode 2, the PV and battery are both the energy sources to drive the SRM. In mode3, the PV is the source and the battery is idle. In mode 4, the battery is the driving source and the PV is idle. In mode 5, the battery is charged by a single-phase grid while both the PV and SRM are idle. In mode 6, the

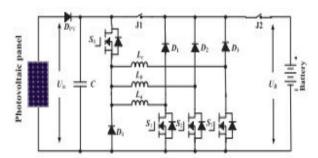battery is charged by the PV and the SRM is idle.

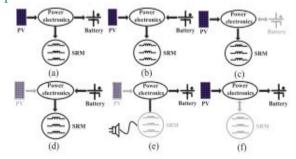Fig. 2. Proposed tri-port topology for PV-powered SRM drive.

Fig. 3. Six operation modes of the proposed tri-port topology. (a) Mode 1. (b) Mode 2. (c) Mode 3. (d) Mode 4. (e) Mode 5. (f) Mode 6

Driving Modes

Operating modes 1–4 are the driving modes to provide traction drive to the vehicle.

1) Mode 1: At light loads of operation, the energy generated from the PV is more than the SRM needed; the system operates in mode 1. The corresponding operation circuit is shown in Fig. 4(a), in which relay J1 turns off and relay J2 turns on. The PV panel energy feeds the energy to SRM and charges the battery; so in this mode, the battery is charged in EV operation condition.

2) Mode 2: When the SRM operates in heavy load such as uphill driving or acceleration, both the PV panel and battery supply power to the SRM. The corresponding operation circuit is shown in Fig. 4(b), in which relay J1 and J2 are turned on.

3) Mode 3: When the battery is out of power, the PV panel is the only energy source to drive

the vehicle. The corresponding circuit is shown in Fig. 4(c). J1 turns on and J2 turns off. When the PV cannot generate electricity due to

4) Mode 4: low solar irradiation, the battery supplies power to the SRM. The corresponding topology is illustrated in Fig. 4(d). In this mode, relay J1 and J2 are both conducting.
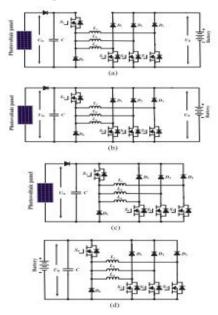

Fig. 2. Equivalent circuits under driving modes. (a) Operation circuit under mode 1. (b) Operation circuit under mode 2. (c) Operation circuit under mode 3. (d) Operation circuit under mode 4.

Battery Charging Modes
Operating modes 5 and 6 are the battery charging modes.

5) Mode 5: When PV cannot generate electricity, an external power source is needed to charge the battery, such as ac grid. The corresponding circuit is shown in Fig. 5(a). J1 and J2 turn on. Point A is central tapped of phase windings that can be easily achieved without changing the motor structure. One of the three-phase windings is split and its midpoint is pulled out, as shown in Fig. 5(a). Phase windings La1 and La2 are employed as input

filter inductors. These inductors are part of the

drive circuit to form an ac–dc rectifier for grid-charging.
6) Mode 6: When the EV is parked under the sun, the PV can charge the battery. J1 turns off and J2 turns on. The corresponding charging circuit is shown in Fig. 5(b).
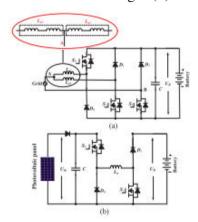

Fig. 3. Equivalent circuits of charging condition modes. (a) Grid charging mode. (b) PV source charging mode.

CONTROL STRATEGY UNDER DIFFERENT MODES
In order to make the best use of solar energy for driving the EV, a control strategy under different modes is designed.

Single Source Driving Mode

According to the difference in the power sources, there are PV-driving, battery-driving, and PV and battery parallel fed source. In a heavy load condition, the PV power cannot support the EV, mode 2 can be adopted to support enough energy and make full use of solar energy. Fig. 6(a) shows the equivalent power source; the corresponding PV panel working points are illustrated in Fig. 6(b).
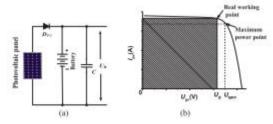

Fig. 4. Power supply at mode 2. (a) Compound power source. (b) Working point of the PV
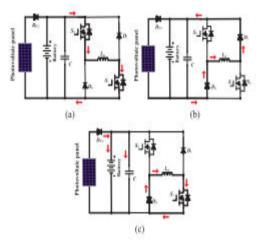
Fig. 5. Working states at mode 2. (a) Winding excitation state. (b) Energy recycling state. (c) Freewheeling state.

Because the PV is paralleled with the battery, the PV panel voltage is clamped to the battery voltage UB. In mode 2, there are three working states: winding excitation, energy recycling, and freewheeling states, as shown in Fig. 7. Modes 3 and 4 have similar working states to mode 2. The difference is that the PV is the only source in mode 3 while the battery is the only source in mode 4. Neglecting the voltage drop across the power switches and diodes, the phase voltage is given by

$$U_{in} = R_k i_k + \frac{d\psi(i_k, \vartheta_r)}{dt}$$
$$= R_k i_k + L_k \frac{di_k}{dt} + i_k \omega_r \frac{dL_k}{d\theta_r}, \quad k = a, b, c \quad (1)$$

where U_{in} is the dc-link voltage, k is phases a, b, or c, R_k is the phase resistance, i_k is the phase current, L_k is the phase inductance, ϑ_r is the rotor position, $\psi(i_k, \vartheta_r)$ is the phase flux linkage depending on the phase current and rotor position, and ω_r is the angular speed.
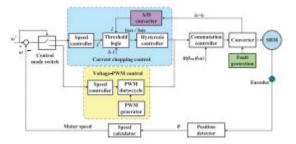

Fig. 6. SRM control strategy under single-source driving mode.

The third term in (1) is the back EMF voltage given by

$$e_k = i_k \omega_r \frac{dL_k}{d\theta_r}. \quad (2)$$

Hence, the phase voltage is found by

$$U_k = R_k i_k + L_k \frac{di_k}{dt} + e_k. \quad (3)$$

In the excitation region, turning on S_0 and S_1 will induce a current in phase a winding, as shown in Fig. 7(a). Phase a winding is subjected to the positive dc bus voltage

$$+U_{in} = R_k i_k + L_k \frac{di_k}{dt} + e_k. \quad (4)$$

When S_0 is OFF and $S1$ is ON, the phase current is in a freewheeling state in a zero-voltage loop, as shown in Fig. 7(c), the phase voltage is zero

$$0 = R_k i_k + L_k \frac{di_k}{dt} + e_k. \quad (5)$$

In the demagnetization region, S_0 and S_1 are both turned off, and the phase current will flow back to the power supply, as shown in Fig. 7(b). In this state, the phase winding is subjected

to the negative dc bus voltage, and the phase voltage is

$$-U_{in} = R_k i_k + L_k \frac{di_k}{dt} + e_k. \quad (6)$$

In single-source driving mode, the voltage-PWM controlis employed as the basic scheme, as illustrated in Fig. 8. According to the given speed $\omega*$, the voltage-PWM control is activated at speed control

Driving-Charging Hybrid Control Strategy

In the driving-charging hybrid control, the PV is the driving source and the battery is charged by the freewheeling current, as illustrated in drive mode 1. There are two control objectives:

MPPT of the PV panel and speed control of the SRM. The dual-source condition is switched from a PV-driving mode. First, the motor speed is controlled at a given speed in mode 3. Then, J2 is turned on and J1 is turned off to switch to mode 1. By controlling the turn-off angle, the maximum power of PV panel can be tracked. There are three steady working states for the dual-source mode (mode 1), as shown in Fig. 9. In Fig. 9(a), S0

and $S1$ conduct, the PV panel charges the SRM winding to drive the motor. In Fig. 9(b), $S0$ and $S1$ turn-off; and the battery is charged with freewheeling current of the phase winding. Fig. 9(c) shows a freewheeling state. Fig. 10 is the control strategy under driving-charging mode. In Fig. 10, ϑon is the turn-on angle of SRM; ϑoff is the turn-off angle of SRM. By adjusting turn-on angle, the speed of SRM can be controlled; the MPPT of PV panel can be achieved by adjusting turn-off angle, which can control the charging current to the battery
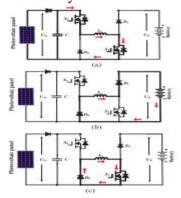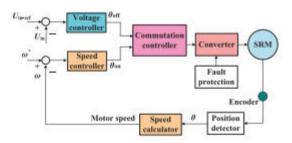

Fig. 7. Mode 1 working states. (a) Winding exciting state. (b) Battery charging state. (c) Freewheeling state

Fig. 8. Control strategy under driving-charging mode (mode 1).

Grid-Charging Control Strategy

The proposed topology also supports the single-phase grid charging. There are four basic charging states and S_0 is always turned off. When the grid instantaneous voltage is over zero, the two working states are presented in Fig. 11(a) and (b). In Fig. 11(a), S_1 and S_2 conduct, the grid voltage charges the phase winding L_{a2}, the corresponding equation can be

expressed as (7); in Fig. 11(b), S_1 turns off and S_2 conducts, the grid is connected in series with phase winding to charges the battery, the corresponding equation can be expressed as (8)

$$U_{grid} = L_{a2} \cdot \frac{di_{grid}}{dt} \qquad (7)$$

$$U_B - U_{grid} = L_{a2} \cdot \frac{di_{grid}}{dt}. \qquad (8)$$

When the grid instantaneous voltage is below zero, the two working states are presented in Fig. 11(c) and (d). In Fig. 11(c), S_1 and S_2 conduct, the grid voltage charges the phase winding L_{a1} and L_{a2}, the corresponding equation can be expressed as (9); in Fig. 11(d), S_1 keeps conducing and S_2 turns off, the grid is connected in series with phase winding L_{a1} and L_{a2} to charges the battery, the corresponding equation can be expressed as (10)

$$U_{grid} = \frac{L_{a1} + L_{a2}}{L_{a1} \cdot L_{a2}} \cdot \frac{di_{grid}}{dt} \qquad (9)$$

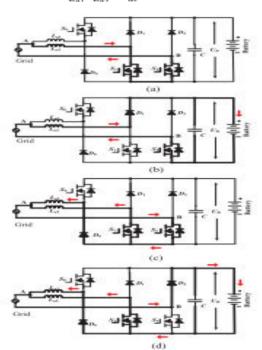$$-U_B - U_{grid} = \frac{L_{a1} + L_{a2}}{L_{a1} \cdot L_{a2}} \cdot \frac{di_{grid}}{dt}. \qquad (10)$$

Fig. 9. Mode 5 charging states. (a) Grid charging state 1 ($U_{grid} > 0$). (b) Grid charging state 2 ($U_{grid} > 0$). (c) Grid charging state 3 ($U_{grid} < 0$). (d) Grid charging state 4 ($U_{grid} < 0$).

In Fig. 12, U_{grid} is the grid voltage; by the phase lock loop (PLL), the phase information can be got; I_{ref_grid} is the given amplitude of the

grid current. Combining sin ϑ and I_{ref_grid}, the instantaneous grid current reference i_{ref_grid} can be calculated. In this mode, when $U_{grid} > 0$, the inductance is L_{a2}; when $U_{grid} < 0$, the inductance is paralleled L_{a1} and L_{a2}; in order to adopt the change in the inductance, hysteresis control is employed to realize grid current regulation. Furthermore, hysteresis control has excellent loop performance, global stability, and small phase lag that make grid-connected control stable.
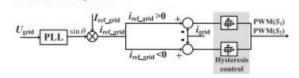

Fig. 12. Grid-connected charging control (mode 5).

PV-Fed Charging Control Strategy

In this mode, the PV panel charges the battery directly by the driving topology. The phase windings are employed as inductor, and the driving topology can be functioned as interleaved buck–boost charging topology. For one phase, there are two states, as shown in Fig. 13(a) and (b). When $S0$ and $S1$ turn on, the PV panel charges phase inductance; when $S0$ and $S1$ turn off, the phase inductance discharges energy to battery. According to the state-of-charging (SoC), there are three stages to make full use of solar energy and maintain battery healthy condition, as illustrated in Fig. 13(c).

During stage 1, the corresponding battery SoC is in SoC0 - SoC1, the battery is in extremely lack energy condition, the MPPT control strategy is employed to make full use of solar energy. During stage 2, the corresponding battery SoC is in SoC1 - SoC2, the constant-voltage control is adopted to charge the battery. During stage 3, the corresponding battery SoC is in SoC2 - 100%, the micro-current charging is adopted. In order to simplify the control strategy, constant voltage is employed in PV panel MPPT control.
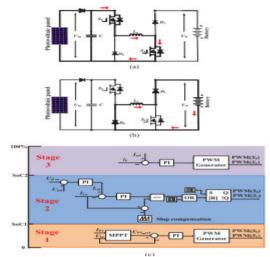

Fig. 10. Mode 6 charging states and control strategy. (a) Phase inductance charging. (b) Battery charging. (c) Charging control strategy.
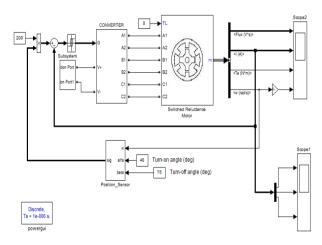
SIMULATION RESULTS

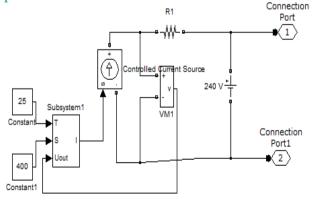Fig. 6.1. Proposed tri-port topology for PV-powered SRM drive.
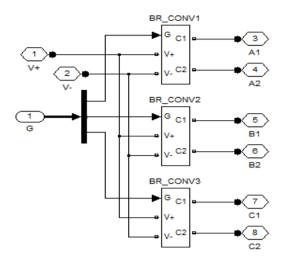

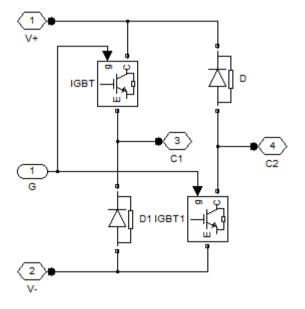Fig 11 Solar subsystem

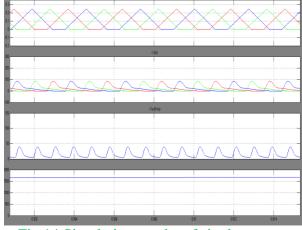Fig 12 Three phase converter

Fig 13 Converter single phase

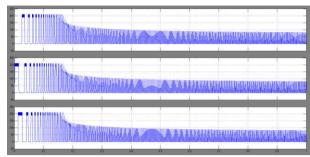Fig 14 Simulation results of single-source driving mode Flux, Current, Torque, Speed

Fig 15 single phase currents

CONCLUSION

In order to tackle the range anxiety of using EVs and decrease the system cost, a combination of the PV panel and SRM is proposed as the EV driving system. The main contributions of this paper are as follows.
1) A tri-port converter is used to coordinate the PV panel, battery, and SRM.
2) Six working modes are developed to achieve flexible energy flow for driving control, driving/charging hybrid control, and charging control.
3) A novel grid-charging topology is formed without a need for external power electronics devices.
4) A PV-fed battery charging control scheme is developed to improve the solar energy utilization. Since PV-fed EVs are a greener and more sustainable technology than conventional ICE vehicles, this work will provide a feasible solution to reduce the total costs and CO_2 emissions of electrified vehicles. Furthermore, the proposed technology may also be applied to similar applications such as fuel cell powered EVs. Fuel cells have a much high-power density and are thus better suited for EV applications

REFERENCES

[1] A. Emadi, L. Young-Joo, and K. Rajashekara, "Power electronics and motor drives in electric, hybrid electric, and plug-in hybrid electric vehicles," IEEE Trans. Ind. Electron., vol. 55, no. 6, pp. 2237–2245, Jun. 2008.
[2] L. K. Bose, "Global energy scenario and

impact of power electronics in 21st century," IEEE Trans. Ind. Electron., vol. 60, no. 7, pp. 2638–2651, Jul. 2013.

[3] J. De Santiago et al., "Electrical motor drivelines in commercial allelectric vehicles: A review," IEEE Trans. Veh. Technol., vol. 61, no. 2, pp. 475–484, Feb. 2012.

[4] Z. Amjadi and S. S. Williamson, "Power-electronics-based solutions for plug-in hybrid electric vehicle energy storage and management systems," IEEE Trans. Ind. Electron., vol. 57, no. 2, pp. 608–616, Feb. 2010.

[5] A. Kuperman, U. Levy, J. Goren, A. Zafransky, and A. Savernin, "Battery charger for electric vehicle traction battery switch station," IEEE Trans. Ind. Electron., vol. 60, no. 12, pp. 5391–5399, Dec. 2013.

[6] S. G. Li, S. M. Sharkh, F. C. Walsh, and C. N. Zhang, "Energy and battery management of a plug-in series hybrid electric vehicle using fuzzy logic," IEEE Trans. Veh. Technol., vol. 60, no. 8, pp. 3571–3585, Oct. 2011.

[7] H. Kim, M. Y. Kim, and G. W. Moon, "A modularized charge equalizer using a battery monitoring IC for series-connected Li-ion battery strings in electric vehicles," IEEE Trans. Power Electron., vol. 28, no. 8, pp. 3779–3787, May 2013.

[8] Z. Ping, Z. Jing, L. Ranran, T. Chengde, and W. Qian, "Magnetic characteristics investigation of an axial–axial flux compound-structure PMSM used for HEVs," IEEE Trans. Magn., vol. 46, no. 6, pp. 2191–2194, Jun. 2010.

[9] A. Kolli, O. Béthoux, A. De Bernardinis, E. Labouré, and G. Coquery, "Space-vector PWM control synthesis for an H-bridge drive in electric vehicles," IEEE Trans. Veh. Technol., vol. 62, no. 6, pp. 2441–2452, Jul. 2013.

[10] Y. Hu, C. Gan, W. Cao, W. Li, and S. Finney, "Central-tapped node linked modular fault tolerance topology for SRM based EV/HEV applications," IEEE Trans. Power Electron., vol. 31, no. 2, pp. 1541–1554, Feb. 2016.

[11] S. M. Yang and J. Y. Chen, "Controlled dynamic braking for switched reluctance motor drives with a rectifier front end," IEEE Trans. Ind. Electron., vol. 60, no. 11, pp. 4913–4919, Nov. 2013.

[12] B. Bilgin, A. Emadi, and M. Krishnamurthy, "Comprehensive evaluation of the dynamic performance of a 6/10 SRM for traction application in PHEVs," IEEE Trans. Ind. Electron., vol. 60, no. 7, pp. 2564–2575, Jul. 2013.

[13] M. Takeno, A. Chiba, N. Hoshi, S. Ogasawara, M. Takemoto, and M. A. Rahman, "Test results and torque improvement of the 50-Kw switched reluctance motor designed for hybrid electric vehicles," IEEE Trans. Ind. Appl., vol. 48, no. 4, pp. 1327–1334, Jul./Aug. 2012.

[14] A. Chiba, M. Takeno, N. Hoshi, M. Takemoto, S. Ogasawara, and M. A. Rahman, "Consideration of number of series turns in switchedreluctance traction motor competitive to HEV IPMSM," IEEE Trans. Ind. Appl., vol. 48, no. 6, pp. 2333–2340, Nov./Dec. 2012.

[15] I. Boldea, L. N. Tutelea, L. Parsa, and D. Dorrell, "Automotive electric propulsion systems with reduced or no permanent magnets: An overview," IEEE Trans. Ind. Electron., vol. 60, no. 9, pp. 5696–5710, Oct. 2014.

[16] X. D. Xue, K. W. E. Cheng, T. W. Ng, and N. C. Cheung, "Multi-objective optimization design of in-wheel switched reluctance motors in electric vehicles," IEEE Trans. Ind. Electron., vol. 57, no. 9, pp. 2980–2987, Sep. 2010.

[17] Y. J. Lee, A. Khaligh, and A. Emadi, "Advanced integrated bidirectional AC/DC and DC/DC converter for plug-in hybrid electric vehicles," IEEE Trans. Veh. Technol., vol. 58, no. 8, pp. 3970–3980, Oct. 2009.

[18] M. Yilmaz and P. T. Krein, "Review of battery charger topologies, charging power levels, and infrastructure for plug-in electric and hybrid vehicles," IEEE Trans. Power Electron., vol. 28, no. 5, pp. 2151–2169, May 2013.

[19] A. Khaligh and S. Dusmez, "Comprehensive topological analysis of conductive and inductive charging solutions for plug-in electric vehicles," IEEE Trans.

Veh. Technol., vol. 61, no. 8, pp. 3475–3489, Oct. 2012.

[20] S. Haghbin, S. Lundmark, M. Alakula, and O. Carlson, "Grid-connected integrated battery chargers in vehicle applications: Review and new solution," IEEE Trans. Ind. Electron., vol. 60, no. 2, pp. 459–473, Feb.2013.

[21] S. Haghbin, S. Lundmark, M. Alakula, and O. Carlson, "An isolated high power integrated charger in electrified-vehicle applications," IEEE Trans. Veh. Technol., vol. 60, no. 9, pp. 4115–4126, Nov. 2011.

[22] S. Haghbin, K. Khan, S. Zhao, M. Alakula, S. Lundmark, and O. Carlson, "An integrated 20-kW motor drive and isolated battery charger for plugin vehicles," IEEE Trans. Power Electron., vol. 28, no. 8, pp. 4013–4029, Aug. 2013.

[23] H. C. Chang and C. M. Liaw, "Development of a compact switchedreluctance motor drive for EV propulsion with voltage-boosting and PFC charging capabilities," IEEE Trans. Veh. Technol., vol. 58, no. 7, pp. 3198–3215, Sep. 2009.

[24] H. C. Chang and C. M. Liaw, "An integrated driving/charging switched reluctance motor drive using three-phase power module," IEEE Trans. Ind. Electron., vol. 58, no. 5, pp. 1763–1775, May 2011.

[25] Y. Hu, X. Song, W. Cao, and B. Ji, "New SR drive with integrated charging capacity for plug-in hybrid electric vehicles (PHEVs)," IEEE Trans. Ind. Electron., vol. 61, no. 10, pp. 5722–5731. Oct. 2014.

[26] Y. Hu, C. Gan, W. Cao, and S. Finney, "Tri-port converter for flexible energy control of PV-fed electric vehicles," in Proc. IEEE Int. Elect. Mach. Drives Conf. (IEMDC'15), Coeur d'Alene, ID, USA, May 10–13, 2015, pp. 1063–1070.